Physiologically Based Pharmacokinetic Modeling of Bergamottin and 6,7-Dihydroxybergamottin to Describe CYP3A4 Mediated Grapefruit-Drug Interactions

Laura Maria Fuhr[1], Fatima Zahra Marok[1], Uwe Fuhr[2], Dominik Selzer[1] and Thorsten Lehr[1,*]

Grapefruit is a moderate to strong inactivator of CYP3A4, which metabolizes up to 50% of marketed drugs. The inhibitory effect is mainly attributed to furanocoumarins present in the fruit, irreversibly inhibiting preferably intestinal CYP3A4 as suicide inhibitors. Effects on CYP3A4 victim drugs can still be measured up to 24 hours after grapefruit juice (GFJ) consumption. The current study aimed to establish a physiologically-based pharmacokinetic (PBPK) grapefruit-drug interaction model by modeling the relevant CYP3A4 inhibiting ingredients of the fruit to simulate and predict the effect of GFJ consumption on plasma concentration-time profiles of various CYP3A4 victim drugs. The grapefruit model was developed in PK-Sim and coupled with previously developed PBPK models of CYP3A4 substrates that were publicly available and already evaluated for CYP3A4-mediated drug–drug interactions. Overall, 43 clinical studies were used for model development. Models of bergamottin (BGT) and 6,7-dihydroxybergamottin (DHB) as relevant active ingredients in GFJ were established. Both models include: (i) CYP3A4 inactivation informed by *in vitro* parameters, (ii) a CYP3A4 mediated clearance estimated during model development, as well as (iii) passive glomerular filtration. The final model successfully describes interactions of GFJ ingredients with 10 different CYP3A4 victim drugs, simulating the effect of the CYP3A4 inactivation on the victims' pharmacokinetics as well as their main metabolites. Furthermore, the model sufficiently captures the time-dependent effect of CYP3A4 inactivation as well as the effect of grapefruit ingestion on intestinal and hepatic CYP3A4 concentrations.

Study Highlights

WHAT IS THE CURRENT KNOWLEDGE ON THE TOPIC?

☑ Grapefruit ingredients are irreversible inactivators of CYP3A4. Furanocoumarins present in the juice are mainly responsible for this effect.

WHAT QUESTION DID THIS STUDY ADDRESS?

☑ The current study aimed to establish a physiologically-based pharmacokinetic (PBPK) model of grapefruit juice (GFJ) ingestion by identifying and explicitly modeling relevant CYP3A4-inhibiting ingredients.

WHAT DOES THIS STUDY ADD TO OUR KNOWLEDGE?

☑ PBPK models of the furanocoumarins bergamottin (BGT) and 6,7-dihydroxybergamottin (DHB) as relevant CYP3A4 inhibitors in grapefruit were successfully developed and coupled to existing PBPK models of CYP3A4 substrates to predict the "grapefruit effect" as well as the effect of furanocoumarin-containing juices from limes and Seville oranges.

HOW MIGHT THIS CHANGE CLINICAL PHARMACOLOGY OR TRANSLATIONAL SCIENCE?

☑ The models support the exploration of "what-if" scenarios, such as: (i) the application of GFJ as "booster" to increase the oral availability of CYP3A4 substrates; (ii) the consideration of GFJ as CYP3A4 inhibitor in clinical studies; (iii) the adjustment of drug doses in patients consuming GFJ; and (iv) the use of the models as a foundation to study drug interactions with furanocoumarin-rich foods.

Grapefruit (*Citrus* × *paradisi*, *Rutaceae*), a citrus fruit with a characteristic bitter-sweet taste, is a hybrid between sweet orange (*Citrus sinensis*) and pomelo (*Citrus maxima*).[1] In the United States, the consumption of pink grapefruit is more popular than white grapefruit.[2] Independent of the variety, 57% of fruits are further processed with grapefruit juice (GFJ) or juice derivatives being a popular product category.[2] However, since the 1970s, the United States consumption of grapefruits

[1]Clinical Pharmacy, Saarland University, Saarbrücken, Germany; [2]Department of Pharmacology, Center for Pharmacology, Faculty of Medicine and University Hospital Cologne, University of Cologne, Cologne, Germany. *Correspondence: Thorsten Lehr (thorsten.lehr@mx.uni-saarland.de)

Received February 7, 2023; accepted May 17, 2023. doi:10.1002/cpt.2968

decreased by about 80% to a per capita consumption of ~0.7 kg in 2018.[2]

The US Food and Drug Administration (FDA) classifies GFJ as a moderate to strong inhibitor of cytochrome P450 (CYP) 3A4,[3] which metabolizes about 50% of marketed drugs.[4] Potential interactions with over 85 different drugs are mentioned in the current literature.[4] Although the FDA classification only considers the juice, the effect is independent of the preparation (whole fruit or juice) or the grapefruit variety. But variety, storage, and differences in juice manufacturing may influence ingredient concentrations.[1] Grapefruit contains a variety of flavonoids and furanocoumarins with the flavonoid naringin being the most abundant ingredient. Flavonoids are assumed to have only a minor contribution to the inhibitory effect after grapefruit consumption, in contrast to furanocoumarins that irreversibly inhibit CYP3A4 as suicide inhibitors.[5,6] Here, the furanocoumarins bergamottin (BGT) and 6,7-dihydroxybergamottin (DHB) are among the most important CYP3A4 inactivators present in grapefruit.[7] The "grapefruit effect" is characterized by a time-dependent CYP3A4 inhibition, lasting more than 24 hours,[8] and by the more pronounced effect on intestinal rather than hepatic CYP3A4.[9,10] Hence, especially drugs with a low oral bioavailability related to CYP3A4 metabolism bear a high risk of interaction.[4] Thereby, one glass of juice (200—250 mL ≙ 1 fruit) might already cause a clinically relevant effect.[4] For example, pronounced increases in felodipine (up to 3.3-fold[9,11]) and simvastatin (up to 18-fold[12]) area under the plasma concentration-time curve (AUC) were observed after GFJ ingestion, which could result in pronounced pharmacodynamic effects or increased risk of adverse effects.[9,12] The consumption of furanocoumarin-containing citrus fruits (e.g., Seville oranges and limes), was also shown to affect drug pharmacokinetics.[13,14]

Clinically relevant interactions with GFJ are listed on drug labels but these listings are often based on the metabolic characteristics of the drug instead of clinical trials.[15] Here, dose-effect models of grapefruit juice-drug interactions (GFJDIs), derived by, for example, physiologically-based pharmacokinetic (PBPK) modeling as a mechanistic modeling technique, could be viable to predict and quantify the effect of grapefruit consumption on the pharmacokinetics and pharmacodynamics of administered drugs and subsequently guide drug labeling. PBPK modeling is accepted by the regulatory agencies, the FDA, and the EMA, with the investigation of drug interactions to support drug clinical study design as a prominent use case.[16] Hence, the presented project aimed to establish a mechanistic PBPK model of grapefruit juice, by modeling its naturally occurring active ingredients BGT and DHB to predict the effect of GFJ ingestion on the pharmacokinetics of CYP3A4 substrates. The GFJDI PBPK model files as well as all the implementation of GFJDIs will be publicly shared with the scientific community on GitHub (http://models.clinicalpharmacy.me).

METHODS

Software

Concentration-time profiles extracted from published clinical studies were digitized with Engauge Digitizer version 12.1 (M. Mitchell,[17] 2020). The PBPK model was developed with PK-Sim and MoBi (Open Systems Pharmacology Suite 9.1, released under the GNU General Public License version 2 (GPLv2) license by the Open Systems Pharmacology community, www.open-systems-pharmacology.org, 2020). Parameter optimization (Monte-Carlo and Levenberg–Marquardt algorithms) and sensitivity analyses were performed with PK-Sim. Pharmacokinetic and statistical analyses as well as plot generation were performed with R version 4.1.3 (The R Foundation for Statistical Computing, Vienna, Austria, 2019).

Literature research and clinical data

Information on the absorption, distribution, metabolism, and elimination (ADME) properties of BGT and DHB as well as information on their inhibition kinetics were derived from literature. Additionally, concentration measurements of these ingredients in GFJ were collected from the literature to analyze typical concentrations as well as the variability of concentrations in the juice. Furthermore, plasma concentration-time profiles of BGT and DHB after GFJ consumption were collected.

Clinical studies investigating the effect of grapefruit consumption on the pharmacokinetics of CYP3A4 victim drugs were collected from the literature. Here, studies were included in the analysis if PBPK models of the victim drugs were available in the Open Systems Pharmacology repository (https://github.com/Open-Systems-Pharmacology/OSP-PBPK-Model-Library) and previously evaluated as CYP3A4 victim drugs in drug–drug interaction predictions. Plasma concentration-time profiles of victim drugs (and their metabolites) with and without administration of GFJ were extracted and digitized from available clinical GFJDI studies. The gathered studies were split into a training dataset for model building and a test dataset for model evaluation. The training dataset was selected to include plasma concentration-time profiles of BGT and DHB and of felodipine with co-administration of isolated BGT and DHB (instead of whole GFJ) to separate the inhibiting effects of both substances. Moreover, the dataset included plasma concentration-time profiles of felodipine and midazolam administered with or after one or multiple glasses of GFJ.

PBPK modeling of grapefruit juice

To establish PBPK models of BGT and DHB, parameter values that could not be informed from the literature were identified by mathematical optimization. Overall, the development of the GFJDI PBPK model was accomplished in a stepwise procedure. First, a set of preliminary drug-dependent parameters of the ingredient models was identified using available plasma concentration-time profiles of the compounds. Subsequently, the preliminary models were coupled to PBPK models of the CYP3A4 victim drugs felodipine[18] and midazolam[19] to simulate the GFJDI studies of the training dataset. The implemented mechanism-based inhibition of CYP3A4 by the ingredients is further described in the **Supplementary Material**, Section 1.2. Based on the simulation results, the preliminary drug-dependent parameter values of the ingredients were further refined and different literature values were tested to parametrize the mechanism-based inhibition of CYP3A4, using the whole training dataset for parameter estimation. Subsequently, the grapefruit interaction PBPK model was used to predict GFJDIs of felodipine and midazolam assigned to the test dataset and GFJDIs with further CYP3A4 victim drugs, namely alfentanil,[19] carbamazepine,[20] itraconazole,[19] verapamil,[21] simvastatin,[22] alprazolam, erythromycin, and triazolam (https://github.com/Open-Systems-Pharmacology/OSP-PBPK-Model-Library). Prior to predicting the GFJDI, the control simulations (without GFJ ingestion) were conducted. Based on the simulation results of the victim drug control, the CYP3A4 k_{cat} of the victim drugs was refined, fitting the simulation to the observed data of the control. The optimized k_{cat} was then used in the GFJDI simulation to predict the interaction.

Grapefruit-drug interaction model evaluation

The performance of the grapefruit PBPK model to predict the effect of GFJDIs was evaluated graphically by comparing (i) predicted victim drug plasma concentration-time profiles without and with GFJ consumption

to those observed in the clinical studies and (ii) predicted GFJDI area under the plasma concentration-time curve from the time of drug administration to the time of the last plasma concentration measurement (AUC_{last}) ratios and GFJDI maximum plasma concentration (C_{max}) ratios to corresponding observed data ratios in goodness-of-fit plots. Geometric mean fold errors (GMFEs) of all GFJDI AUC_{last} and C_{max} ratios were calculated as quantitative performance metrics. The model evaluation is described in more detail in the **Supplementary Material**, Section 1.1.

RESULTS

In total, 43 clinical studies were used for the development of the grapefruit PBPK model, providing 118 mean and 3 median plasma concentration-time profiles of the victim drugs felodipine, midazolam, alprazolam, triazolam, carbamazepine, alfentanil, erythromycin, itraconazole, simvastatin, and verapamil (50 control profiles, 71 GFJDI profiles) as well as 42 plasma concentration-time profiles of their metabolites (18 control profiles, 24 GFJDI profiles). Overall, a broad spectrum of GFJDI scenarios was investigated. Victim drugs were applied: (i) orally or intravenously, (ii) once or repeatedly, and (iii) together with GFJ or 0–144 hours after juice consumption. GFJ was administered (iv) as single- or double-strength preparation (1:3 or 1:1 dilution of juice concentrate with water) or grapefruit segments or ethanolic extract from segment-free parts, (v) in volumes of 200–300 mL, and (vi) in single or multiple doses before victim drug administration. Additionally, 2 studies investigated (vii) the effect of different doses of BGT or (viii) DHB on felodipine plasma concentration-time profiles. Last, two studies investigated (ix) the effect of Seville orange juice and (x) lime juice on felodipine pharmacokinetics. A detailed description of all clinical studies is provided in the **Supplementary Material**, Section 3. An overview of the modeling workflow and the developed GFJDI network is provided in **Figure 1**.

PBPK models of BGT and DHB were established and consumption of GFJ was simulated as oral administration of the respective compounds. To determine the ingested doses of these compounds, information on the administered juice volume and the concentration of ingredients in GFJ is required. As concentrations of BGT and DHB contained in the GFJ were only measured for 13 of 71 and 11 of 71 investigated scenarios, additional concentration measurements were gathered from the literature and all available concentration measurements were analyzed. Overall, reported doses were highly variable, ranging from 0.50 to 94.56 µmol/L (mean [± SD]: 18.49 [± 14.04]) for BGT and from 0.80 to 132.57 µmol/L (mean [± SD]: 28.9 [± 33.23]) for DHB and differed among the available juice preparations, as illustrated in **Figure 2a,b**, respectively. Mean DHB concentrations measured in juice prepared from frozen concentrate (mean [± SD]: 25.1 µmol/L [± 20.48], $n = 20$) were significantly higher (t-test; $P = 0.00637$) than those measured in canned juice (mean [± SD]: 9.92 µmol/L [± 10.58], $n = 20$). For BGT concentrations, differences in frozen concentrate (mean [± SD]: 18.7 [± 6.66], $n = 20$) and canned juice (mean [± SD]: 16.63 [± 20.4], $n = 19$) were not statistically significant (t-test; $P = 0.677$). The complete analysis of reported ingredient concentrations is described in the **Supplementary Material**, Section 2.1. Mean concentrations of BGT and DHB for each juice preparation obtained from the available measurements were used to calculate administered doses in the administered GFJ if the clinical study did not provide concentration measurements.

BGT and DHB exhibit similar ADME properties. Both furanocoumarins are of moderate lipophilicity and presumably well absorbed from the intestines.[5] It is assumed that both compounds undergo extensive metabolic elimination and that enzyme inactivation is mediated by reactive metabolites.[23] Hence, the BGT and DHB PBPK models include: (i) a CYP3A4-mediated clearance process, (ii) mechanism-based inhibition of CYP3A4, and (iii) free glomerular filtration. The mechanism-based inactivation of CYP3A4 was parametrized using literature values. The CYP3A4-mediated clearance was described using Michaelis–Menten kinetics. As no measurements of the CYP3A4 metabolism were available in the literature, the inhibition constant (K_I) was used as a surrogate for the Michaelis–Menten constant and the catalytic rate constant was estimated. Other drug-dependent parameters were either taken from the literature (e.g., molecular weight, pK_a, solubility, and fraction unbound), calculated within PK-Sim (e.g., cellular permeabilities) or optimized (e.g., specific intestinal permeability and lipophilicity). All drug-dependent parameters used in the final models are listed in **Table 1**. Predicted vs. observed plasma concentration-time profiles of both ingredients are illustrated in **Figure 2c,d**, thereby the plasma concentration-time profiles for BGT and DHB are sufficiently described, with average GMFE values of 1.53 and 1.02 for AUC_{last}, and 1.10 and 1.08 for C_{max} of DHB and BGT, respectively. The corresponding AUC_{last} and C_{max} values can be found in **Table S5**, whereas goodness-of-fit plots of predicted vs. observed: (i) AUC_{last}, (ii) C_{max}, and (iii) plasma concentration values are depicted in **Figure S5**.

Overall, the ingredient models successfully described the effect of grapefruit intake on various CYP3A4 victim drugs. **Figure 3** displays predicted vs. observed plasma concentration-time profiles of different victim drugs and their metabolites (if metabolite models were available) of exemplary studies with and without the consumption of GFJ.

Figure 4 illustrates predicted compared with observed plasma concentration-time profiles of the victim drug felodipine and illustrates the versatility of the ingredient models to describe different scenarios. Felodipine is the drug in which the "grapefruit effect" was observed first and which subsequently was used extensively as a probe drug to further assess the GFJDI in clinical studies. The models describe the GFJDI with felodipine: (i) after intravenous or after oral administration of felodipine with GFJ (ii) ingested once or repeatedly, (iii) ingested with or up 24 hours before felodipine, and administered as (iv) single- or double-strength preparation. Furthermore, the model predicts the effect of (v) individual grapefruit ingredients or (vi) Seville orange or (vii) lime juice on felodipine plasma concentrations. Compared with the effect of one glass of single-strength GFJ on oral felodipine, the model successfully predicts the lack of effect on intravenously applied felodipine (**Figure 4a**), a 55% (observed: 46%) higher felodipine AUC_{last} if GFJ was ingested over several days before felodipine administration (**Figure 4c**) as well

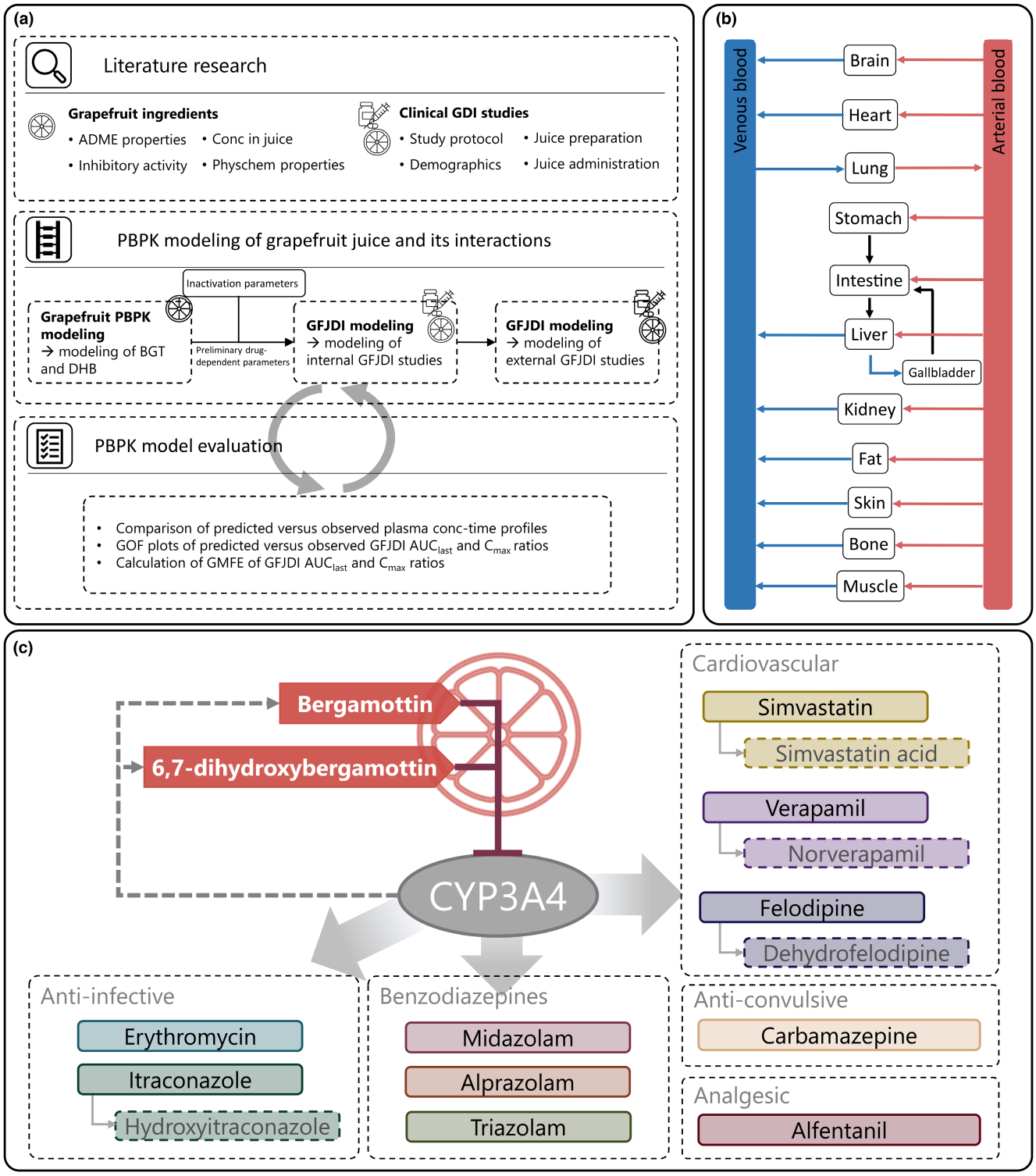

Figure 1 Modeling workflow and model overview. (**a**) The modeling process can be divided into literature research on GFJ and its active ingredients, model development of GFJ ingredients and its interactions and model evaluation. (**b**) Overview of the PBPK model structure. Different compartments represent ADME-relevant organs of the body. Connections between compartments represent arterial and venous blood flow. (**c**) The final GFJDI model describes mechanism-based inhibition of CYP3A4 by BGT and DHB to cover the effect of GFJ and includes a broad range of CYP3A4 victim drugs along with their metabolites. ADME, absorption, distribution, metabolism, and excretion; AUC, area under the plasma concentration-time curve; BGT, bergamottin; C_{max}, maximum plasma concentration; conc, concentration; CYP3A4, cytochrome P450 3A4; DHB, 6,7-dihydroxybergamottin; GFJDI, grapefruit juice-drug interaction; GMFE, geometric mean fold error; GOF, goodness-of-fit; PBPK, physiologically-based pharmacokinetic.

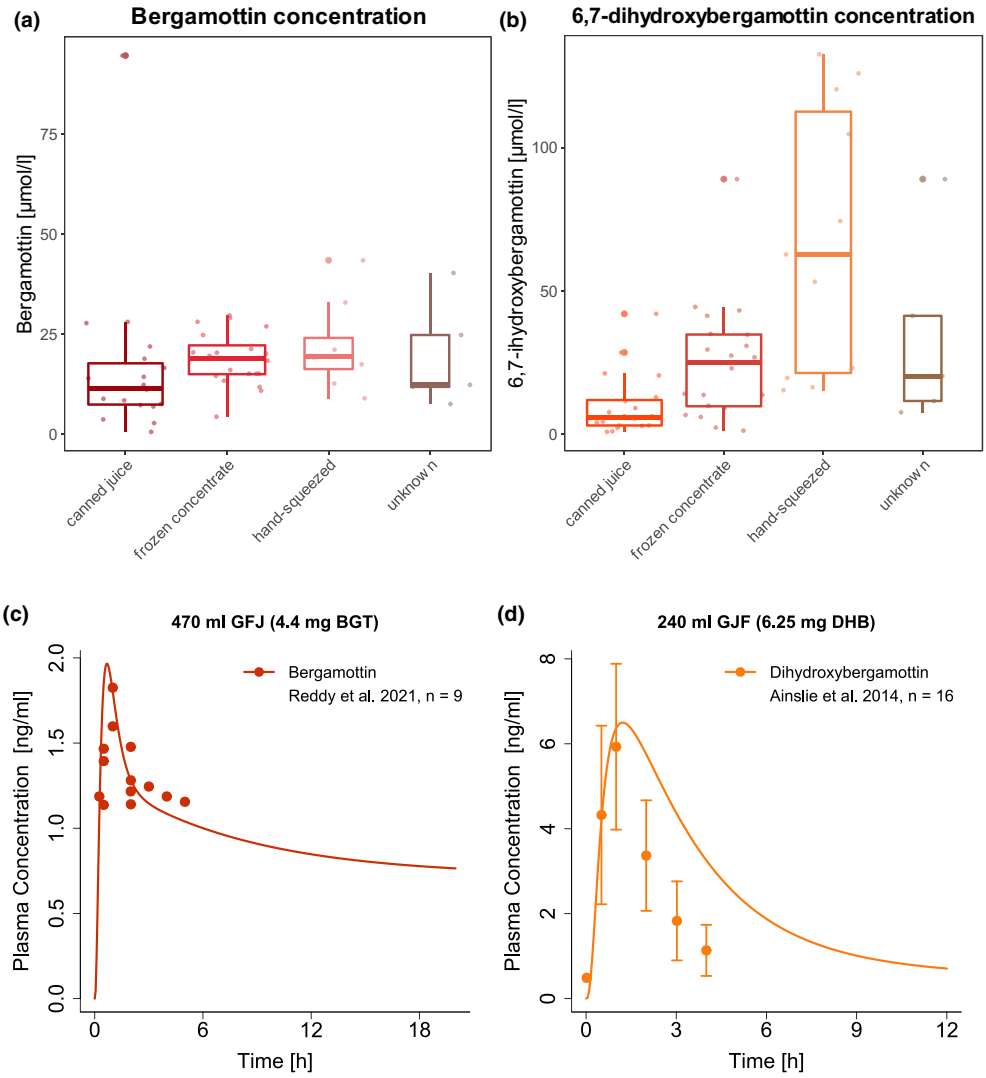

Figure 2 Concentration measurements of (**a**) BGT and (**b**) DHB in different GFJ preparations. Boxplots show the following descriptive statistics: The median value, the IQR, and the 1.5-fold IQR, as well as individual measurements (small dots) and potential outliers (big dot; at least 1.5 IQR greater than the third quartile); as well as predicted vs. observed plasma concentration-time profiles of (**c**) BGT and (**d**) DHB. Solid lines represent model predictions while the different shapes represent observed data. BGT, bergamottin; DHB, 6,7-dihydroxybergamottin; GFJ, grapefruit juice; IQR, interquartile range; K_i, concentration for half-maximal inactivation; *n*: number of participants.

as a 10% (observed: 19%) higher felodipine AUC_{last} if double-strength GFJ was administered (**Figure 4f**). Furthermore, the performance of the BGT and DHB model was investigated by simulating the inhibiting effect of single ingredients and by simulating the effect of juices of limes (**Figure 4j**) and Seville oranges (**Figure 4k**). In the corresponding clinical studies, BGT and DHB concentrations of 5 and 36 µmol/L were determined in Seville oranges, whereas concentrations in GFJ were 16 and 23 µmol/L, respectively.[13] Pure lime juice contained 100 µmol/L BGT and no DHB and was diluted to ¼ strength, whereas the administered GFJ contained 25 µmol/L BGT (DHB concentrations not indicated).[14] Solely the effect of grapefruit segments (**Figure 4i**; blended segments without flavedo, albedo, and vascular elements) and extract (segment-free parts extracted with ethanol) could not be sufficiently described.

The impact of different juice types, and consequently ingredient concentrations, was examined for alprazolam. In this case, the effects of canned juice (BGT: 1.13 mg, DHB: 0.74 mg) and juice from frozen concentrate (BGT: 1.27, DHB: 1.87 mg) were analyzed to investigate if the grapefruit effect may be more potent when using a frozen concentrate preparation. A moderate increase in the effect on alprazolam AUC (up to 25%) was observed if frozen concentrate was used compared with canned juice.

Plasma concentration-time profiles of all clinical studies included in the PBPK modeling analysis are depicted in the **Supplementary Material**, Section 3. The overall model performance is illustrated in **Figure 5a,b** in goodness-of-fit plots of predicted compared with observed GFJDI AUC_{last} and C_{max} ratios of victim drugs and their metabolites of all included clinical studies. Overall, mean (range) GMFE values of 1.30 (1.00–3.66) and 1.31 (1.00–3.08) were calculated for GFJDI AUC_{last} and C_{max} ratios, respectively, with 93% of predicted GFJDI AUC_{last} and C_{max} ratios deviating less than 2-fold from the corresponding observed values.

Table 1 Drug-dependent parameters of bergamottin and 6,7-dihydroxybergamottin

		Bergamottin			6,7-dihydroxybergamottin		
Parameter	Unit	Model	Literature	Ref	Model	Literature	Ref
MW	g/mol	338.4 (lit)	338.4	[46]	372.417 (lit)	372.417	[47]
log*P*		4.95 (opt)	4.81, 5.3	[46]	3.72 (opt)	2.67, 3.4	[47]
pK_a		—	—	—	13.84 (lit)	13.84	[47]
$f_{u,plasma}$	%	2.73 (calc)	2.73	[48]	7.70 (calc)	7.70	[48]
Solubility	mg/L	10 (7) (lit)	10 (7)	[46]	44 (7) (lit)	44 (7)	[47]
K_m (CYP3A4)	µmol/L	1.9 (asm)	—	—	1.10 (asm)	—	—
k_{cat} (CYP3A4)	1/minute	0.05 (opt)	—	—	2.10 (opt)	—	—
GFR fraction		1 (asm)	—	—	1 (asm)	—	—
K_I (CYP3A4)	µmol/L	1.9 (lit)	1.9–40	[6,29,49]	1.10 (lit)	1.1–59	[6,49,50]
k_{inact} (CYP3A4)	1/minute	0.70 (lit)	0.08–0.70	[6,29,49]	0.41 (lit)	0.06–0.52	[6,49,50]
K_i (CYP3A4)	µmol/L	6.10 (lit)	0.5–13.3	[6]	0.50 (lit)	0.4–0.9	6
Intestinal permeability	cm/minute	1.60 E-3 (opt)	—	—	6.41 E-5 (opt)	—	—

asm, assumed; calc, calculated; GFR, glomerular filtration rate; k_{cat}, catalytic rate constant; K_I, concentration for half-maximal inhibition; K_I, concentration for half-maximal inhibition k_{inact} maximum inactivation rate constant; K_m, Michaelis–Menten constant; lit, literature; log*P*, lipophilicity; MW, molecular weight; opt, optimized; pK_a, acid dissociation constant.

The effect of GFJ on CYP3A4 exhibits two key characteristics. First, BGT and DHB are irreversible inhibitors of CYP3A4, resulting a time-dependent CYP3A4 inhibition, lasting more than 24 hours. Consequently, the effects of GFJ on victim drug pharmacokinetics can be observed even if the victim drug is taken 24 hours after grapefruit consumption, which is sufficiently covered by the model as shown in **Figure 4d,e**. Second, the CYP3A4 inhibition is more pronounced in the intestine, whereas hepatic CYP3A4 is only affected after frequent juice consumption over several days. Overall, the model successfully described the effect of GFJ ingestion on oral drug bioavailability and successfully simulated the decreased intestinal CYP3A4 metabolism, as illustrated in **Figure 5c** comparing predicted to observed GFJDI bioavailability and intestinal availability (F_G) ratios. The effect of intestinal and hepatic CYP3A4 inhibition by GFJ simulated with the model is exemplarily shown for midazolam as a victim drug. **Figure 6a** depicts predicted compared with observed plasma concentration-time profiles of midazolam with or without the ingestion of one glass of GFJ (single- or double-strength), whereas **Figure 6b** shows plasma concentration-time profiles of midazolam without or after consumption of a total of 6 glasses of GFJ for 2 days prior to midazolam administration. The model sufficiently described the effect of GFJ ingestion on midazolam plasma concentration-time profiles in all 3 cases and predicted a 276% (observed: 276%) higher midazolam AUC for the consumption of 6 glasses compared with one glass of GFJ. Furthermore, marked increases in midazolam terminal half-life ($t_{1/2}$) could be observed if the drug was administered after multiple doses of GFJ but not for co-administration with a single glass of GFJ. As illustrated in **Figure 5d**, comparing predicted to observed GFJDI $t_{1/2}$ ratios, the model was able to describe the effect of single and multiple doses of GFJ on midazolam, felodipine, and triazolam $t_{1/2}$.

To further investigate the difference in the effect magnitude of GFJ on duodenal vs. hepatic CYP3A4, the model was applied to predict CYP3A4, BGT, and DHB concentrations in the duodenum and liver during administration of one glass of juice (**Figure 6**, left column) or multiple glasses of juice (**Figure 6**, right column). For the ingestion of one glass of juice, the model predicts maximum hepatic ingredient concentrations below K_I, whereas concentrations close to or above K_I are predicted for frequent GFJ ingestion. Ingredient concentrations in the duodenum exceed K_I by several fold for single and frequent juice ingestion. Subsequently, the model predicts a strong decrease in intestinal CYP3A4, independent of frequency of juice consumption, as well as a frequency-dependent decrease in hepatic CYP3A4.

DISCUSSION

In the presented analysis, a GFJDI PBPK model was successfully established and evaluated. The model describes the consumption of GFJ as oral administration of the furanocoumarins BGT and DHB and successfully describes and predicts CYP3A4-mediated GFJDIs for a broad spectrum of victim drugs and scenarios.

Models of BGT and DHB were established as important CYP3A4 inactivators in grapefruit, regarding: (i) their abundance in the juice as well as (ii) their inactivation activity.[7] *In vivo* studies could show that a naringin solution[24] or furanocoumarin-free GFJ[25] did not markedly impact felodipine pharmacokinetics, implying that furanocoumarins are the main CYP3A4 inactivators in GFJ. However, the inhibitory effects of BGT and DHB observed *in vivo* were slightly smaller compared with the effect of whole GFJ.[26,27] Hence, the effect cannot be attributed to one of these ingredients alone. Overall, CYP3A4 inactivation by grapefruit is complex and may result from a combination of ingredients present in the juice.[7] This may explain why the current grapefruit model covering solely BGT and DHB could not sufficiently describe the administration of GFJ ethanol extract and homogenized segments. This may be related to altered ingredient concentrations in respective preparations, and thus an altered

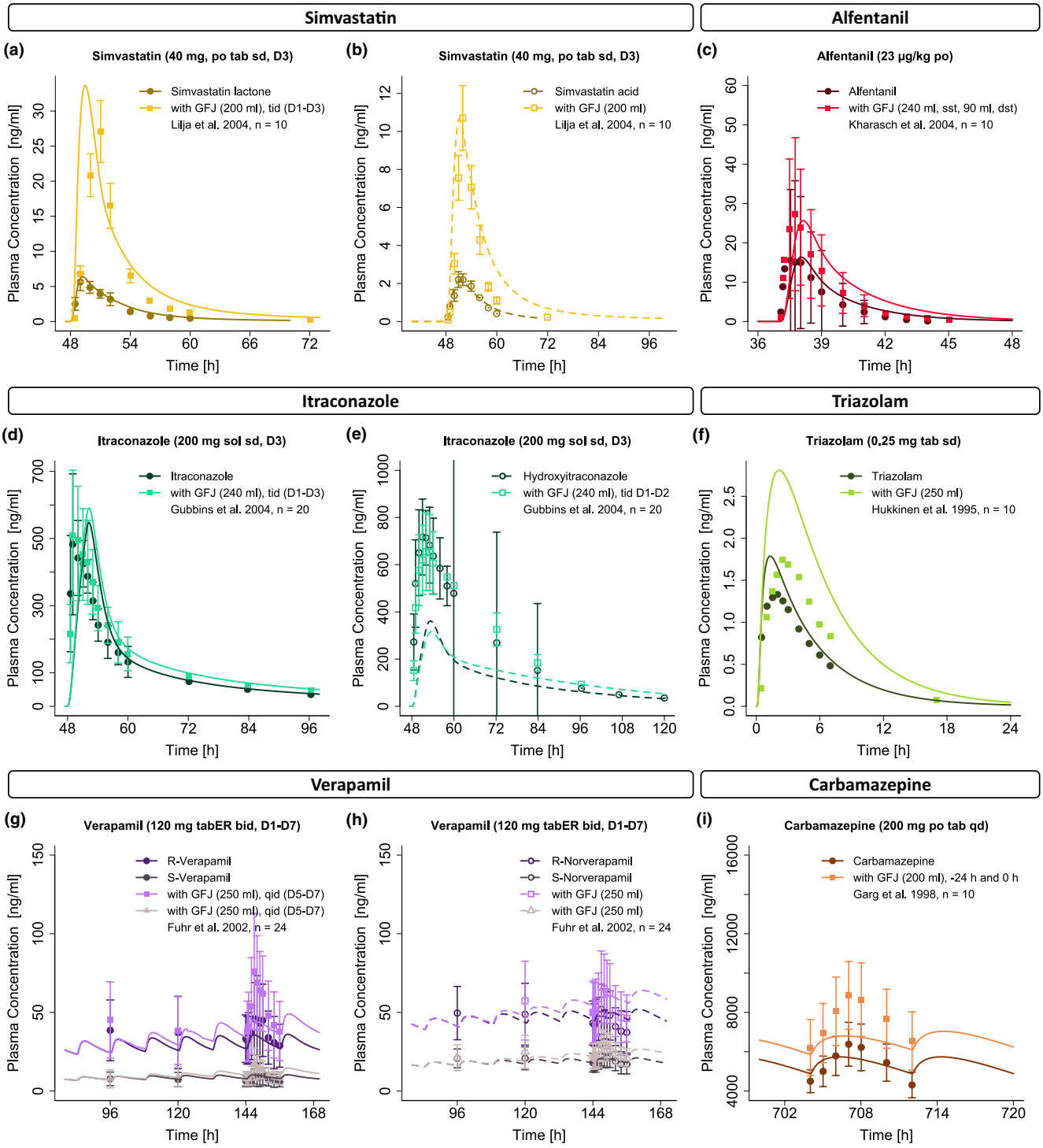

Figure 3 Comparison of predicted and observed victim drug plasma concentration-time profiles with and without the administration of GFJ of (**a**) simvastatin and (**b**) its metabolite simvastatin acid,[12] (**c**) alfentanil,[39] (**d**) itraconazole, and (**e**) its metabolite hydroxyitraconazole,[40] (**f**) triazolam,[41] (**g**) R- and S-verapamil, and (**h**) their metabolites R- and S-norverapamil,[42] (**i**) carbamazepine.[43] Lines represent model predictions while the different shapes represent observed data (± SD, if available). D, day; d, double strength; GFJ, grapefruit juice; iv, intravenous; *n*, number of participants; po, oral, qd, once daily; s, single strength; sd, single dose; sol, solution; tab, tablet; tabER, extended-release tablet; tid, three times daily.

contribution of the ingredients to the grapefruit effect. For example, naringin concentrations in the ethanol extracts were ninefold higher compared with GFJ. Even though naringin and/or its metabolite naringenin does not strongly contribute to the CYP3A4 inhibition at concentrations measured in GFJ, it is conceivable that especially naringenin may additionally impact victim drug concentrations at such high concentrations.[5] The characterization of the pharmacokinetics of BGT and DHB has been challenging

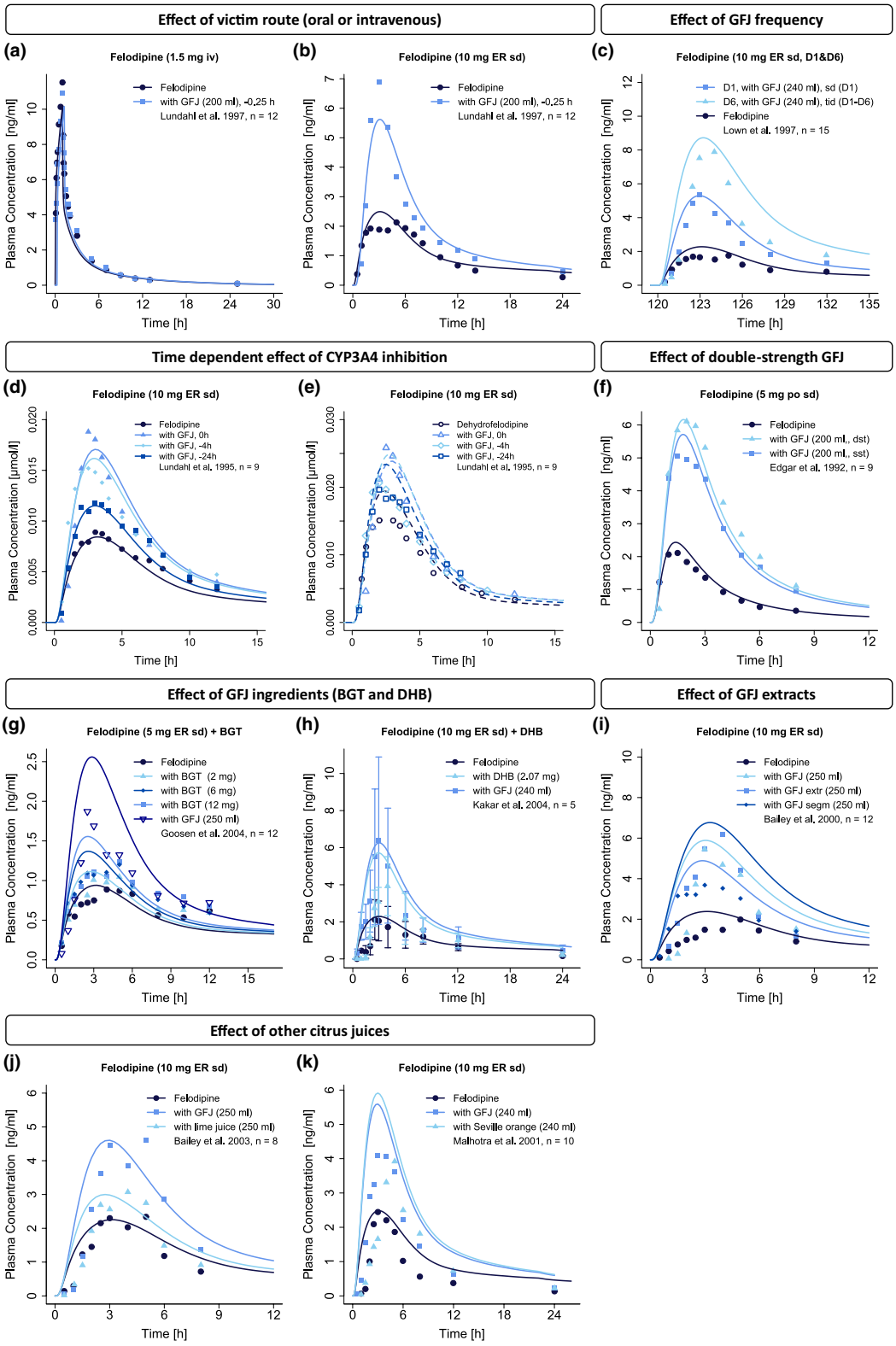

due to the limited information on their metabolism and concentration measures in the human body. Within the scope of the presented analysis, the models were developed to describe GFJDIs with CYP3A4 victim drugs. As more comprehensive information becomes available, these models can be easily refined.

Overall, CYP3A4-mediated GFJDIs are highly variable. First, this can be related to the high interindividual variability of intestinal CYP3A4, where up to an 8-fold difference in intestinal concentrations was reported.[28] Second, it should be considered that grapefruit is a natural product and the concentration of ingredients

Figure 4 Comparison of predicted and observed felodipine drug plasma concentration-time profiles with and without administration of GFJ (**a**) after intravenous administration or (**b**) oral administration of felodipine,[9] (**c**) with and without the administration of GFJ (frequently administered or a single glass), (**d**) with and without grapefruit ingestion concomitantly, 4 hours or 24 hours before felodipine administration along with corresponding (**e**) dehydrofelodipine plasma concentration-time profiles (**f**) with and without the administration of double- or single-strength GFJ[11] (**g**) with and without the administration of different doses of BGT (2–12 mg) compared with GFJ,[26] (**h**) with and without the administration of juice "serum" (aqueous supernatant of frozen concentrate suspended in water, containing primarily DHB) compared with GFJ,[27] as well as (**i**) blended segments (segments) and ethanol extract from segment free parts (extract)[44] and (**j**) with and without the administration of lime juice[14] or (**k**) Seville orange[13] in comparison to GFJ. Lines represent model predictions, whereas the different shapes represent observed data (± SD, if available). BGT, bergamottin; D, day; d, double strength; DHB, 6,7-dihydroxybergamottin; ER, extended-release formulation; extr, extract; GFJ, grapefruit juice; iv, intravenous; *n*, number of participants; po, oral; s, single strength; sd, single dose; segm, segments; sol, solution; tab, tablet; tid, three times daily.

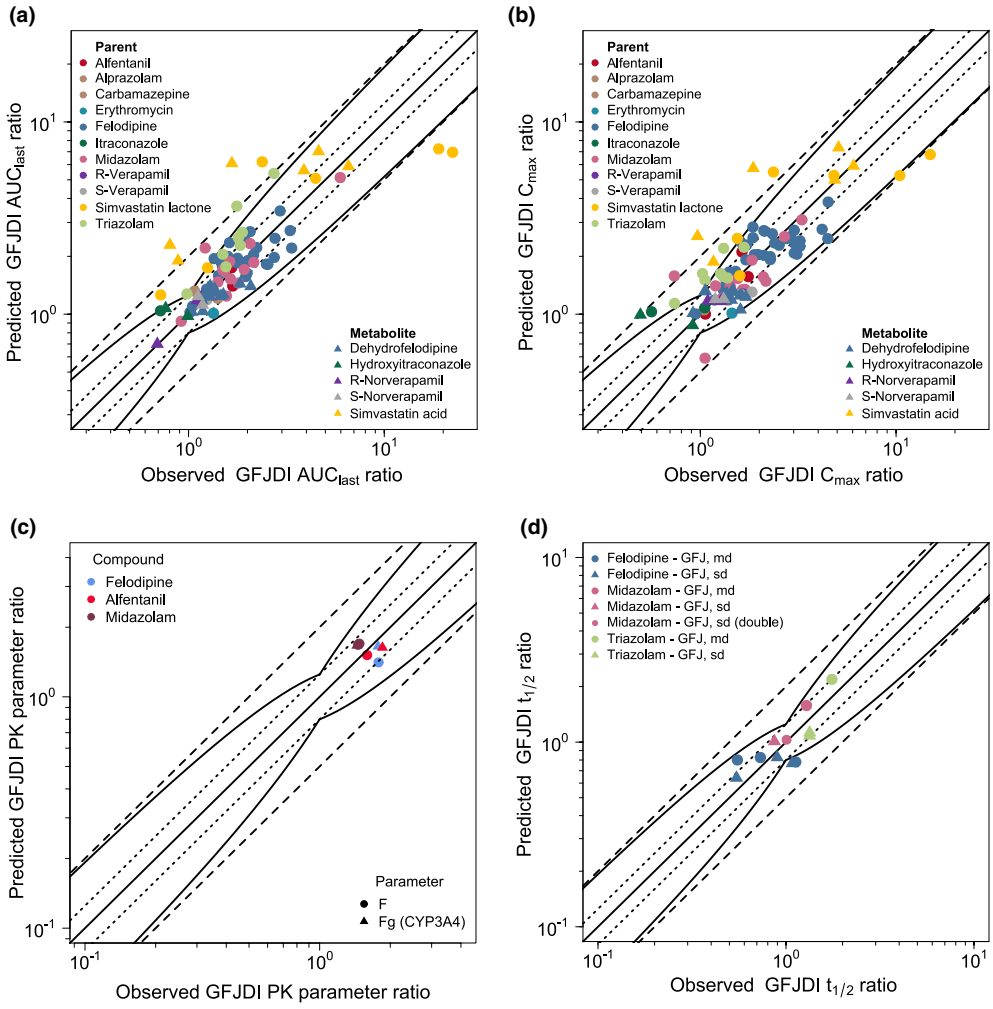

Figure 5 Performance of the GFJDI model. The performance of the model to predict the effect on the included victim drugs is illustrated in goodness-of-fit plots, comparing predicted versus observed (**a**) GFJDI AUC_{last} ratios and (**b**) GFJDI C_{max} ratios of all GFJDI studies as well as (**c**) GFJDI bioavailability and F_g ratios and (**d**) GFJDI $t_{1/2}$ ratios of selected studies. The line of identity is shown as a straight solid line; the curved solid lines mark the prediction success limits proposed by Guest et al.[45] A 1.25-fold deviation is shown as dotted lines; a 2-fold deviation is shown as dashed lines. Details on the GFJDI studies and all references are provided in the **Supplementary Material**, Section 3. AUC_{last}, area under the plasma concentration–time curve from dosing to the last concentration measurement; C_{max}, maximum plasma concentration; F, oral bioavailability; F_g, intestinal availability; GFJ, grapefruit juice; GFJDI, grapefruit–drug interaction; PK, pharmacokinetic; $t_{½}$, terminal half-life.

may vary[7] depending, for example, on external growing conditions and the fruit variety. Storage and processing of the fruit can also influence the concentrations.[1] A high variability of BGT and DHB concentrations in GFJ with differences of more than 100-fold could be observed during the analysis of ingredient concentrations reported in the literature. For ~80% of the simulated scenarios, the ingredient concentrations were not indicated in the clinical study but had to be assumed based on the administered juice preparation to estimate the ingested dose. Even though in most cases the true concentration of BGT and DHB was unknown, the model sufficiently described and predicted GFJDIs for different victim drugs assuming mean ingredient concentrations which is supported by

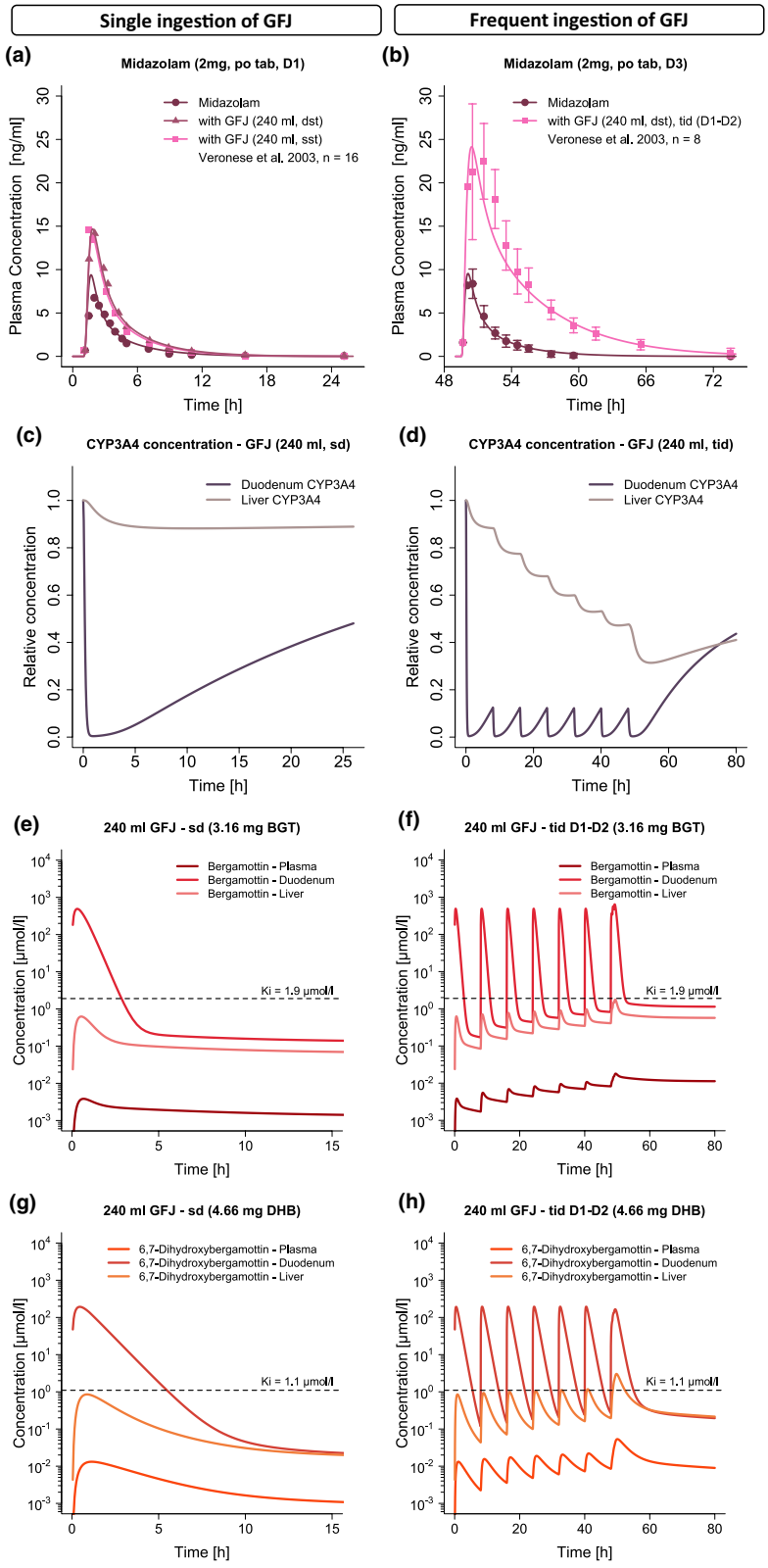

Figure 6 Effect of grapefruit on intestinal and hepatic CYP3A4. Comparison of predicted and observed (**a, b**) midazolam plasma concentration-time profiles, (**c, d**) predicted duodenum and liver CYP3A4 concentrations and predicted (**e, f**) BGT and (**g, h**) DHB concentrations in plasma, duodenum and liver after oral administration of midazolam with and without concomitant consumption of one glass of single- or double-strength GFJ (left column) or after consumption of GFJ over 2 days before midazolam administration (right column).[10] BGT, bergamottin; CYP3A4, cytochrome P450; d, double-strength; DHB, 6,7-dihydroxybergamottin; GFJ, grapefruit juice; GFJDI, grapefruit-drug interaction; D, day; po, oral; tab, tablet; *n*, number of participants; s, single-strength; sd, single dose; tid, three times daily.

mean calculated GMFEs of 1.30 and 1.31 for GFJDI AUC_{last} and C_{max} ratios. This may be due to the fact that the effect is almost completely established after the consumption of 200 mL of juice, and doubling the dose of perpetrator moieties (e.g., by administering double-strength juice), does not considerably impact the effect.[10,11] However, regarding the pronounced variability, specifying ingredient concentrations in future studies would enhance comparability between studies and improve comprehension of the grapefruit effect. Although GFJDIs with triazolam are generally well-described (GMFE GFJDI AUC_{last} ratio = 1.49; GFJDI GMFE C_{max} ratio = 1.40), the model tends to overpredict the effect of GFJ, which cannot be solely attributed to high variability in CYP3A4 and juice ingredients. Given that GFJDIs with the structurally related CYP3A4 substrate midazolam are sufficiently described (GMFE GFJDI AUC_{last} ratio = 1.17; GMFE GFJDI C_{max} ratio = 1.24), it is plausible to assume that the overprediction of the effect could also result from an inadequate description of intestinal CYP3A4 metabolism of triazolam.

The current model only reflects the inhibition of CYP3A4. However, inhibition of further metabolic and transport proteins besides CYP3A4 is reported.[29] For verapamil, transport via P-glycoprotein (P-gp) may be considered, however, clinical studies with digoxin as sensitive P-gp victim drug showed that grapefruit ingestion did not impact P-gp-mediated transport.[30] For simvastatin and erythromycin, transport via OATP may also be impacted by GFJ. Plasma concentrations of simvastatin lactone and its metabolite simvastatin acid were adequately predicted for co-administration with single-strength GFJ. However, when co-administrated with double-strength juice, the predicted grapefruit effect deviated from the observed effect. In this case, it cannot be ruled out that concentrations of other ingredients, such as naringin, might be high enough to markedly impact the transport of simvastatin. For example, it has been demonstrated that the flavonoid naringin can impair OATP-mediated transport of pravastatin and pitavastatin.[31] Carbamazepine is additionally metabolized via CYP2C8 and CYP2B6.[20] Even though grapefruit has been shown to inhibit CYP2B6 as well,[23] the current simulation, only considering CYP3A4 inhibition, adequately describes the grapefruit-carbamazepine interaction. This is demonstrated by GMFEs of GFJDI AUC_{last} and C_{max} ratios of 1.16 and 1.17, respectively. Hereby, the model describes the complex interaction with carbamazepine as a victim and autoinducer of CYP3A4, whereby CYP3A4 is mutually induced and inhibited.

The two key characteristics of the "grapefruit effect"—the time-dependent CYP3A4 inhibition, lasting more than 24 hours, and the predominant intestinal inhibition—were well-captured by the model. The time-dependent CYP3A4 inhibition could be described using inhibition parameters from the literature, demonstrated by the sufficient prediction of felodipine and dehydrofelodipine plasma concentration-time profiles, if felodipine was administered simultaneously, or up to 24 hours after GFJ.[8] The CYP3A4 inhibition is primarily limited to intestinal CYP3A4, whereas only frequent juice consumption causes hepatic CYP3A4 inhibition.[10] The model reasonably described this characteristic by predicting: (i) the lack of effect of one glass of juice on intravenous victim drugs, (ii) the effect on oral bioavailability and F_g, and (iii) the effect on drug $t_{1/2}$. Based on model predictions of BGT, DHB, and CYP3A4 concentrations in the duodenum and liver, concentrations of the ingredients in the liver after the consumption of one glass of juice are well below K_I and, thus, insufficient to inactivate CYP3A4. In contrast, predicted duodenal ingredient concentrations are severalfold above K_I and a strong decrease in intestinal CYP3A4 concentrations is predicted, independently of the frequency of GFJ ingestion.

Additional PBPK modeling approaches to describe the "grapefruit effect" are available in the literature. These approaches aimed to describe the "grapefruit effect "either mechanistically by modeling BGT[32] or DHB as active ingredients,[33,34] or non-mechanistically by adjusting intestinal CYP3A4 concentrations, gastric emptying time,[35] or V_{max}.[36,37] The herein presented analysis included a particularly large set of clinical studies ($n = 43$), investigating 10 different CYP3A4 victim drugs as well as their metabolites. Thereby, the model was thoroughly challenged and used to extensively investigate the unique features of the "grapefruit effect." The GFJDI model sufficiently describes: (i) the effect on intravenously and orally applied victim drugs, (ii) the effect on oral bioavailability and F_G, (iii) the impact on drug $t_{1/2}$ for single vs. repeated grapefruit consumption, (iv) the effect on victim drug metabolite plasma concentration-time profiles, and (v) the time-dependent effect of the CYP3A4 inhibition. In addition, no other modeling approach aimed to predict the effect of GFJ by modeling both active ingredients—BGT and DHB—although the effect cannot be attributed to one of these ingredients alone. Furthermore, the models of BGT and DHB could be successfully applied to predict the effects of Seville orange and lime juice consumption on the pharmacokinetics of felodipine. Both furanocoumarins are found in several commonly consumed fruits and their respective juices, herbs, and vegetables (e.g., parsley, different citrus fruits but also celeriac and parsnip).[38] Here, the developed PBPK models could provide the basis to investigate the effects of additional furanocoumarin-containing foods on CYP3A4 substrates.

In summary, a grapefruit PBPK model was successfully developed and the effect of GFJ on various victim drugs could be described by modeling ingestion of GFJ as oral administration of the active ingredients BGT and DHB. The selection of modeled GFJDIs was based on the availability of victim drug PBPK models within the Open Systems Pharmacology Suite as well as clinical studies providing plasma concentration-time profiles in the literature. However, the GFJDI model can be easily adapted to predict GFJDIs with additional CYP3A4 substrates, such as buspirone, lovastatin, or tacrolimus,[3] which may also provide further insights into the performance of the presented grapefruit model. Moreover, the model could also be utilized to investigate dosing adjustments and provide a building block to investigate potential effects of furanocoumarins in foods. Additionally, the model can also be used for educational purposes to illustrate the pronounced effect that the consumption of GFJ might have on a patient's medication.

SUPPORTING INFORMATION

Supplementary information accompanies this paper on the *Clinical Pharmacology & Therapeutics* website (www.cpt-journal.com).

FUNDING

This research was funded by the German Federal Ministry of Education and Research (BMBF), grant number 031L0161C ("OSMOSES").

ACKNOWLEDGMENT

Open Access funding enabled and organized by Projekt DEAL.

CONFLICT OF INTEREST

T.L. has received research grants from the German Federal Ministry of Education and Research (grant 031L0161C). All other authors declared no competing interests for this work. The funders had no role in the design of the study; in the collection, analyses, or interpretation of data; in the writing of the manuscript, or in the decision to publish the results.

AUTHOR CONTRIBUTIONS

L.M.F., F.Z.M., U.F., D.S., and T.L. wrote the manuscript. L.M.F., F.Z.M., and T.L. designed the research. L.M.F. performed the research. L.M.F., F.Z.M., and D.S. analyzed the data.

1. Hung, W.L., Suh, J.H. & Wang, Y. Chemistry and health effects of furanocoumarins in grapefruit. *J. Food Drug Anal.* **25**, 71–83 (2017).
2. Chen, L.A. & House, L. An overview of the grapefruit market in the U.S. *EDIS* **2021**, 1–7 (2021).
3. U.S. Food and Drug Administration. Drug development and drug interactions. Table of substrates, inhibitors and inducers. <https://www.fda.gov/drugs/drug-interactions-labeling/drug-development-and-drug-interactions-table-substrates-inhibitors-and-inducers>. Accessed March 31, 2023.
4. Bailey, D.G., Dresser, G. & Arnold, J.M.O. Grapefruit-medication interactions: forbidden fruit or avoidable consequences? *CMAJ* **185**, 309–316 (2013).
5. Fuhr, U. Drug interactions with grapefruit juice. Extent, probable mechanism and clinical relevance. *Drug Saf.* **18**, 251–272 (1998).
6. Paine, M.F., Criss, A.B. & Watkins, P.B. Two major grapefruit juice components differ in intestinal CYP3A4 inhibition kinetic and binding properties. *Drug Metab. Dispos.* **32**, 1146–1153 (2004).
7. Guo, L.Q., Fukuda, K., Ohta, T. & Yamazoe, Y. Role of furanocoumarin derivatives on grapefruit juice-mediated inhibition of human CYP3A activity. *Drug Metab. Dispos.* **28**, 766–771 (2000).
8. Lundahl, J., Regårdh, C.G., Edgar, B. & Johnsson, G. Relationship between time of intake of grapefruit juice and its effect on pharmacokinetics and pharmacodynamics of felodipine in healthy subjects. *Eur. J. Clin. Pharmacol.* **49**, 61–67 (1995).
9. Lundahl, J., Regårdh, C.G., Edgar, B. & Johnsson, G. Effects of grapefruit juice ingestion-pharmacokinetics and haemodynamics of intravenously and orally administered felodipine in healthy men. *Eur. J. Clin. Pharmacol.* **52**, 139–145 (1997).
10. Veronese, M.L. *et al*. Exposure-dependent inhibition of intestinal and hepatic CYP3A4 in vivo by grapefruit juice. *J. Clin. Pharmacol.* **43**, 831–839 (2003).
11. Edgar, B., Bailey, D., Bergstrand, R., Johnsson, G. & Regårdh, C.G. Acute effects of drinking grapefruit juice on the pharmacokinetics and dynamics of felodipine—and its potential clinical relevance. *Eur. J. Clin. Pharmacol.* **42**, 313–317 (1992).
12. Lilja, J.J., Neuvonen, M. & Neuvonen, P.J. Effects of regular consumption of grapefruit juice on the pharmacokinetics of simvastatin. *Br. J. Clin. Pharmacol.* **58**, 56–60 (2004).
13. Malhotra, S., Bailey, D.G., Paine, M.F. & Watkins, P.B. Seville orange juice-felodipine interaction: comparison with dilute grapefruit juice and involvement of furocoumarins. *Clin. Pharmacol. Ther.* **69**, 14–23 (2001).
14. Bailey, D.G., Dresser, G.K. & Bend, J.R. Bergamottin, lime juice, and red wine as inhibitors of cytochrome P450 3A4 activity: comparison with grapefruit juice. *Clin. Pharmacol. Ther.* **73**, 529–537 (2003).
15. Huang, S.M. *et al*. Drug interactions with herbal products and grapefruit juice: a conference report. *Clin. Pharmacol. Ther.* **75**, 1–12 (2004).
16. European Medicines Agency. Guideline on the investigation of drug interactions. <https://www.ema.europa.eu/en/documents/scientific-guideline/guideline-investigation-drug-interactions-revision-1_en.pdf> (2015). Accessed April 4, 2023.
17. Mitchell, M., Muftakhidinov, B. & Winchen, T. Engauge Digitizer Software. <http://markummitchell.github.io/engauge-digitizer> Accessed March 22, 2023.
18. Fuhr, L.M., Marok, F.Z., Mees, M., Mahfoud, F., Selzer, D. & Lehr, T. A physiologically based pharmacokinetic and Pharmacodynamic model of the CYP3A4 substrate Felodipine for drug–drug interaction modeling. *Pharmaceutics* **14**, 1474 (2022).
19. Hanke, N. *et al*. PBPK models for CYP3A4 and P-gp DDI prediction: a modeling network of rifampicin, itraconazole, clarithromycin, midazolam, alfentanil, and digoxin. *CPT Pharmacometr. Syst. Pharmacol.* **7**, 647–659 (2018).
20. Fuhr, L.M., Marok, F.Z., Hanke, N., Selzer, D. & Lehr, T. Pharmacokinetics of the CYP3A4 and CYP2B6 inducer carbamazepine and its drug-drug interaction potential: a physiologically based pharmacokinetic modeling approach. *Pharmaceutics* **13**, 1–21 (2021).
21. Hanke, N. *et al*. A mechanistic, enantioselective, physiologically based pharmacokinetic model of verapamil and Norverapamil, built and evaluated for drug-drug interaction studies. *Pharmaceutics* **12**, 556 (2020).
22. Wojtyniak, J., Selzer, D., Schwab, M. & Lehr, T. Physiologically based precision dosing approach for drug-drug-gene interactions: a simvastatin network analysis. *Clin. Pharmacol. Ther.* **109**, 201–211 (2021).
23. Kent, U.M., Lin, H.L., Noon, K.R., Harris, D.L. & Hollenberg, P.F. Metabolism of bergamottin by cytochromes P450 2B6 and 3A5. *J. Pharmacol. Exp. Ther.* **318**, 992–1005 (2006).
24. Bailey, D.G., Arnold, J.M., Munoz, C. & Spence, J.D. Grapefruit juice--felodipine interaction: mechanism, predictability, and effect of naringin. *Clin. Pharmacol. Ther.* **53**, 637–642 (1993).
25. Paine, M.F. *et al*. A furanocoumarin-free grapefruit juice establishes furanocoumarins as the mediators of the grapefruit juice-felodipine interaction. *Am. J. Clin. Nutr.* **83**, 1097–1105 (2006).
26. Goosen, T.C. *et al*. Bergamottin contribution to the grapefruit juice-felodipine interaction and disposition in humans. *Clin. Pharmacol. Ther.* **76**, 607–617 (2004).
27. Kakar, S.M., Paine, M.F., Stewart, P.W. & Watkins, P.B. 6′7′-Dihydroxybergamottin contributes to the grapefruit juice effect. *Clin. Pharmacol. Ther.* **75**, 569–579 (2004).
28. Sica, D.A. Interaction of grapefruit juice and calcium channel blockers. *Am. J. Hypertens.* **19**, 768–773 (2006).
29. He, K., Iyer, K.R., Hayes, R.N., Sinz, M.W., Woolf, T.F. & Hollenberg, P.F. Inactivation of cytochrome P450 3A4 by bergamottin, a component of grapefruit juice. *Chem. Res. Toxicol.* **11**, 252–259 (1998).
30. Parker, R.B., Yates, C.R., Soberman, J.E. & Laizure, S.C. Effects of grapefruit juice on intestinal P-glycoprotein: evaluation using digoxin in humans. *Pharmacotherapy* **23**, 979–987 (2003).
31. Shirasaka, Y., Suzuki, K., Nakanishi, T. & Tamai, I. Differential effect of grapefruit juice on intestinal absorption of statins due to inhibition of organic anion transporting polypeptide and/or P-glycoprotein. *J. Pharm. Sci.* **100**, 3843–3853 (2011).
32. Pilla Reddy, V., Jo, H. & Neuhoff, S. Food constituent– and herb–drug interactions in oncology: influence of quantitative modelling on drug labelling. *Br. J. Clin. Pharmacol.* **87**, 3988–4000 (2021).

33. Fenneteau, F., Poulin, P. & Nekka, F. Physiologically based predictions of the impact of inhibition of intestinal and hepatic metabolism on human pharmacokinetics of CYP3A substrates. *J. Pharm. Sci.* **99**, 486–514 (2010).
34. Ainslie, G. R. A translational approach to assess the risk of dietary substance-drug interactions [doctoral dissertation, University of North Carolina]. Carolina Digital Repository. (2014). https://doi.org/10.17615/9ynp-bg55
35. Wagner, C., Thelen, K., Willmann, S., Selen, A. & Dressman, J.B. Utilizing In vitro and PBPK tools to link ADME characteristics to plasma profiles: case example Nifedipine immediate release formulation. *J. Pharm. Sci.* **102**, 3205–3219 (2013).
36. Pepin, X.J.H. *et al*. Bridging in vitro dissolution and in vivo exposure for acalabrutinib. Part II. A mechanistic PBPK model for IR formulation comparison, proton pump inhibitor drug interactions, and administration with acidic juices. *Eur. J. Pharm. Biopharm.* **142**, 435–448 (2019).
37. Marsousi, N. *et al*. Coadministration of ticagrelor and ritonavir: toward prospective dose adjustment to maintain an optimal platelet inhibition using the PBPK approach. *Clin. Pharmacol. Ther.* **100**, 295–304 (2016).
38. Melough, M.M. *et al*. Identification and quantitation of Furocoumarins in popularly consumed foods in the U.S. using QuEChERS extraction coupled with UPLC-MS/MS analysis. *J. Agric. Food Chem.* **65**, 5049–5055 (2017).
39. Kharasch, E.D., Walker, A., Hoffer, C. & Sheffels, P. Intravenous and oral alfentanil as in vivo probes for hepatic and first-pass cytochrome P450 3A activity: noninvasive assessment by use of pupillary miosis. *Clin. Pharmacol. Ther.* **76**, 452–466 (2004).
40. Gubbins, P.O. *et al*. Influence of grapefruit juice on the systemic availability of itraconazole oral solution in healthy adult volunteers. *Pharmacotherapy* **24**, 460–467 (2004).
41. Hukkinen, S.K., Varhe, A., Olkkola, K.T. & Neuvonen, P.J. Plasma concentrations of triazolam are increased by concomitant ingestion of grapefruit juice. *Clin. Pharmacol. Ther.* **58**, 127–131 (1995).
42. Fuhr, U. *et al*. Effects of grapefruit juice and smoking on verapamil concentrations in steady state. *Eur. J. Clin. Pharmacol.* **58**, 45–53 (2002).
43. Garg, S.K., Kumar, N., Bhargava, V.K. & Prabhakar, S.K. Effect of grapefruit juice on carbamazepine bioavailability in patients with epilepsy. *Clin. Pharmacol. Ther.* **64**, 286–288 (1998).
44. Bailey, D.G., Dresser, G.K., Kreeft, J.H., Munoz, C., Freeman, D.J. & Bend, J.R. Grapefruit-felodipine interaction: effect of unprocessed fruit and probable active ingredients. *Clin. Pharmacol. Ther.* **68**, 468–477 (2000).
45. Guest, E.J., Aarons, L., Houston, J.B., Rostami-Hodjegan, A. & Galetin, A. Critique of the two-fold measure of prediction success for ratios: application for the assessment of drug-drug interactions. *Drug Metab. Dispos.* **39**, 170–173 (2011).
46. Human Metabolome Database. Metabocard for bergamottin (HMDB0033782). <https://hmdb.ca/metabolites/HMDB0033782> (2022). Accessed January 31, 2023.
47. Human Metabolome Database. Metabocard for 6,7-dihydroxybergamottin (HMDB0039066). <https://hmdb.ca/metabolites/HMDB0039066> (2022). Accessed January 31, 2023.
48. Watanabe, R. *et al*. Predicting fraction unbound in human plasma from chemical structure: improved accuracy in the low value ranges. *Mol. Pharm.* **15**, 5302–5311 (2018).
49. Tassaneeyakul, W., Guo, L.Q., Fukuda, K., Ohta, T. & Yamazoe, Y. Inhibition selectivity of grapefruit juice components on human cytochromes P450. *Arch. Biochem. Biophys.* **378**, 356–363 (2000).
50. Schmiedlin-Ren, P. *et al*. Mechanisms of enhanced oral availability of CYP3A4 substrates by grapefruit constituents: decreased enterocyte CYP3A4 concentration and mechanism-based inactivation by furanocoumarins. *Drug Metab. Dispos.* **25**, 1228–1233 (1997).